Surface-Plasmon-Assisted Guiding of Broadband Slow and Subwavelength Light in Air

Aristeidis Karalis,* E. Lidorikis, Mihai Ibanescu, J. D. Joannopoulos, and Marin Soljačić

Center for Materials Science and Engineering and Research Laboratory of Electronics, Massachusetts Institute of Technology, Cambridge, Massachusetts 02139, USA

(Received 23 April 2005; published 2 August 2005)

A class of axially uniform waveguides is introduced, employing a new mechanism to guide light inside a low-index dielectric material without the use of photonic band gap, and simultaneously exhibiting subwavelength modal size and very slow group velocity over an unusually large frequency bandwidth. Their basis is the presence of plasmonic modes on the interfaces between dielectric regions and the flat unpatterned surface of a bulk metallic substrate. These novel waveguides allow for easy broadband coupling and exhibit absorption losses limited only by the intrinsic loss of the metal.

DOI: 10.1103/PhysRevLett.95.063901 PACS numbers: 42.82.Et, 73.20.Mf, 78.20.Ci, 78.68.+m

Precise control of the properties of light propagation along linear waveguides has always been of great importance in the world of optics. One challenging goal has been to guide light through air in the presence of higher-refractive-index dielectric media, since light tends to localize itself mostly in these high-index regions. So far, photonic band gaps [1] and other index-guiding based mechanisms [2] have been ways to address this issue. Another very desirable attribute for modern nanophotonics is the transverse confinement of guided light in subwavelength-size regions. Such compact guidance has been accomplished by exploring surface-plasmon modes [3] into designing waveguides, by using conductors of a finite cross section [4–8], combinations of surface plasmons with band gaps [9], or coupled-metallic-nanoparticle chains [10]. Finally, great effort has been focused recently on slowing down light [11], but so far the proposed systems have the undesirable characteristic of a fairly small frequency bandwidth, which is often described as a fundamental limit to the achievable delay-bandwidth product [12]. In this Letter, we introduce a new class of axially uniform waveguides that simultaneously accomplish all the desired properties discussed above. They are implemented on a simple flat conducting surface of a large extent and rely on a nonperiodic dielectric distribution on top of this substrate to generate transversely confined guided modes. The new mechanism for confining much more field in the low-index region rather than in the adjacent high-index region is based on the relative dispersive characteristics of different surface-plasmon modes present in these structures and is applicable within a finite but wide frequency regime that abides by certain cutoff conditions. Supporting subwavelength modal sizes is a common property of all surface-plasmon structures. Similarly, supporting very slow group velocities over unusually large frequency bandwidths is a unique physical property inherent to most *layered* plasmonic structures, that is, to our knowledge, pointed out here for the first time and extended to linear waveguides. The promises of the proposed systems in the field of nanophotonics are exciting, including a significant reduction in all (spatial, temporal, and operational energy) device scales. These novel waveguides can easily be coupled to other systems and exhibit propagation losses minimized to the limit set by the intrinsic loss of the metallic substrate.

Surface plasmons (SP) are well known [3] electromagnetic waves that propagate along the interface between a dielectric material and a metal of permittivities ϵ and ϵ_p. The conditions for the existence of a SP are TM polarization (magnetic field parallel to the interface) and $\epsilon_p < -\epsilon < 0$. For example, with $\epsilon_p(\omega) = 1 - \omega_p^2/\omega^2$, where ω_p is the bulk plasma frequency, these conditions lead to a high frequency cutoff at $\omega_c(\epsilon) = \omega_p/\sqrt{1+\epsilon}$. The dispersion relation $k = \omega/c\sqrt{\epsilon \cdot \epsilon_p(\omega)/[\epsilon + \epsilon_p(\omega)]}$ is shown by curves A and B in Fig. 1 for two different dielectric materials ($\epsilon_{\text{hi}} > \epsilon_{\text{low}}$ in insets A and B).

Several extensions of this simple structure in the form of planar layers have been examined in the past [13,14]. As

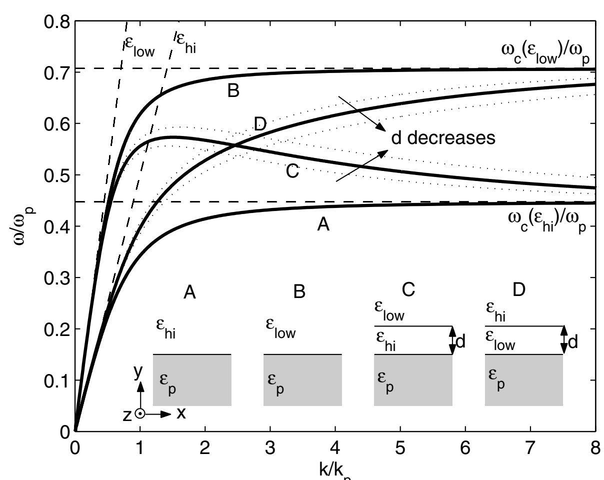

FIG. 1. ω-k diagrams (solid curves) for conventional layered surface-plasmon structures (insets A–D) with $\epsilon_{\text{hi}} = 4$ and $\epsilon_{\text{low}} = 1$ (air). Layer thicknesses $d/\lambda_p = 0.015$, 0.02, and 0.025 are used for C and D (solid + dotted curves). The light lines $\omega/\omega_p = \sqrt{\epsilon}k/k_p$ ("vertical" dashed lines) and the cutoff frequencies $\omega_c(\epsilon)/\omega_p = 1/\sqrt{1+\epsilon}$ (horizontal dashed lines) are shown.

motivation for the designs that follow, let us consider here the case of a $\epsilon_{\rm hi}$-dielectric layer of thickness d inserted between a $\epsilon_{\rm low}$-dielectric space and the plasmonic material ϵ_p (Fig. 1, inset C). The dispersion relation of the mode (curve C) is implicitly determined by $\tanh(u_{\rm hi}\epsilon_{\rm hi}d) = -(1 + u_p/u_{\rm low})/(u_{\rm hi}/u_{\rm low} + u_p/u_{\rm hi})$, where $u_{\rm hi} = \epsilon_{\rm hi}^{-1}\sqrt{k^2 - \omega^2/c^2\epsilon_{\rm hi}}$ and similarly for $u_{\rm low}$ and u_p. The localization of the mode to the metal-$\epsilon_{\rm hi}$ interface increases with the wave vector k. Therefore, for low frequencies ω (and small k) the mode has most of its energy stored in the outer dielectric $\epsilon_{\rm low}$, and thus follows the behavior of a SP in $\epsilon_{\rm low}$ (curve B), while in the limit of large k the mode does not "see" much of the outside material, and thus must asymptote to the SP in $\epsilon_{\rm hi}$ (curve A). The smaller the thickness d the higher the wave number k where this change in behavior happens, as depicted in Fig. 1 with dotted curves. Furthermore, for d smaller than a certain threshold, the mode exhibits a regime of *negative* group velocity. Similarly, if the two dielectric materials are interchanged (inset D), there still exists a vertically confined (namely, exponentially decaying as $|y| \to \infty$) surface wave (curve D), which now has opposite asymptotic behavior from C in the two limits of low ω and high k values, so its group velocity is always *positive*.

A significant remark for both cases is that sufficiently decreasing the layer thickness can lead to arbitrarily small group velocity (negative or positive, respectively) over the *entire large bandwidth* $[\omega_c(\epsilon_{\rm hi}), \omega_c(\epsilon_{\rm low})]$, and actually with small group velocity dispersion. This is a unique physical property for layered plasmonic systems, since any other known system that can support very low group velocities (such as electromagnetically induced transparency or a photonic crystal) does so only within a narrow frequency band. This striking attribute of unlimited "frequency bandwidth over group velocity" ratio carries over immediately to linear plasmonic waveguides, such as the ones discussed below.

All of the above surface plasmons are vertically (along y) confined, but infinitely extended in the x-z plane of propagation. We would like to design linear, axially uniform waveguides that can support modes guided along z [with $\exp(i\beta z - i\omega t)$ dependence], but confined also in the lateral x direction. Consider, for the x-y cross section of such a waveguide, a semi-infinite vertical slab of width w and permittivity $\epsilon_{\rm low}$, placed on top of the semi-infinite space of conducting medium ϵ_p, and surrounded by a higher-index medium $\epsilon_{\rm hi}$, as shown in inset (i) of Fig. 2(a). If we divide this waveguide cross section into three vertical slices, then the central slice has an average dielectric permittivity lower than that of the exterior slices. Thus, one might expect that light confinement in x is not possible, by invoking the common index-guiding mechanism. However, we now show that this structure, devoid of a photonic band gap or a finite-sized conductor, supports well-defined guided modes with the desired property of having much more energy stored inside the $\epsilon_{\rm low}$ slab rather than the neighboring $\epsilon_{\rm hi}$ space. The central slice, if examined individually being uniform in x-z, supports the SP B from Fig. 1, which lies in the ω-k plane above the SP A, supported by the high-index outer slices. Let now SP B travel inside the plasma-$\epsilon_{\rm low}$ slice at a small angle with the z axis (namely, with a large $k_z = \beta$ component of its total wave vector k_B). Then, upon incidence on the $\epsilon_{\rm hi}$ boundary (uniform in z), it couples to A only for frequencies below $\omega_c(\epsilon_{\rm hi})$, in which case, in order to preserve β phase matching along z, A has to radiate outwards in x (since $\beta < k_B < k_A \Rightarrow k_{x,A}^2 = k_A^2 - \beta^2 > 0$), excluding, indeed, the possibility for the existence of confined guided modes. However, above this cutoff the SP mode A disappears, and the lowest order mode of the outer slices that can lead to radiation laterally or vertically becomes just the first mode within the continuum described by the $\epsilon_{\rm hi}$ light line. This line now lies above the SP B ($\omega/c\sqrt{\epsilon_{\rm hi}} < k_B$) for a *narrow* frequency range below $\omega_c(\epsilon_{\rm low})$, so B can now couple only to decaying modes inside the high-index side claddings. Thus in this frequency regime fully transversely confined guided modes can exist, with propagation con-

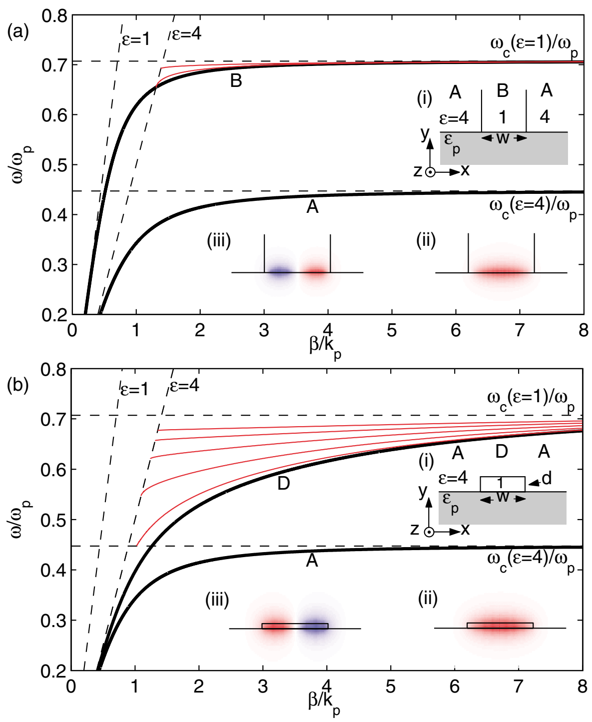

FIG. 2 (color). ω-β diagrams (red curves calculated via the effective-index method) for SP-based waveguide structures [insets (i)] with $w/\lambda_p = 0.25$ and $d/\lambda_p = 0.02$. The SP modes A–D (from Fig. 1) of the individual vertical slices (thick solid black curves) and the $\epsilon_{\rm hi}$ light line (dashed black curve) limit the regions where fully confined modes can exist. The H_x component of the first two modes at (a) $\omega/\omega_p = 0.705$ and (b) $\omega/\omega_p = 0.65$ is shown [insets (ii) and (iii) calculated via a finite-difference frequency-domain eigenmode solver].

stants β between the $\epsilon_{\rm hi}$ light line and B, and with a significant part of the energy stored inside the low-index core. To our knowledge, this is a new guiding mechanism that is enabled by the unique cutoff properties of SP modes.

A simple method to quickly obtain an estimate for the propagation constants β_n of the guided modes is the effective-index method [15]: each ith vertical slice is replaced by a homogeneous dielectric layer of refractive index equal to the effective index $[n_{{\rm eff},i} = k_i/(\omega/c)]$ of the lowest order mode $(k_i, \phi_i(y))$ supported within this slice; the complicated cross section of the waveguide thus gets reduced into a simpler but approximately equivalent dielectric layered structure, whose modes can easily be found, making sure that the most appropriate polarization of the fields is used. The method is most accurate when the transverse profiles $\phi_i(y)$ of these lowest order modes are nearly the same, so that the couplings to higher order modes can be safely ignored. To implement the method for the structure of Fig. 2(a), the effective indices of the SPs B and A should be used, respectively, for the central and outer layers of the resulting symmetric slab waveguide, while the E field is chosen to be polarized along y, since B and A are TM polarized with the H field in the x-z plane. The resulting dispersion curves are shown in Fig. 2(a). An infinite number of modes is found just below the $\omega = \omega_c(\epsilon_{\rm low})$ cutoff line, since in that frequency region $k \rightarrow \infty$, for curve B, so the effective slab waveguide is one with an infinite index contrast, which indeed supports an infinite number of modes inside its core. The effective-index method is within 1% accuracy for the fundamental mode by comparison to "exact" (but technically difficult) simulations with a finite-difference frequency-domain (FDFD) eigenmode solver for a few frequencies. The exact TM-like H_x component of the first two modes is shown in insets (ii) and (iii) and is, indeed, found to be 2 orders of magnitude larger than the TE-like components.

The case in which the central low-permittivity slab has a finite height d is shown as inset (i) in Fig. 2(b) and can be treated similarly. The only difference here is that the inner slice alone supports the SP D from Fig. 1, which still lies above the SP A for $\omega < \omega_c(\epsilon_{\rm hi})$, but below the $\epsilon_{\rm hi}$ light line, the lowest order mode supported by the sides for $\omega_c(\epsilon_{\rm hi}) < \omega < \omega_c(\epsilon_{\rm low})$. Therefore, for a fixed frequency ω within this *broad* range, guided modes exist with wave numbers β between the $\epsilon_{\rm hi}$ light line and D, since only in this regime is the field composed only by decaying modes in the outer regions. The effective-index method indicates how the dispersion curves approximately look [Fig. 2(b)], while the FDFD modes are again shown in insets (ii) and (iii).

For completeness, let us examine also the case where the values of the dielectrics for the structures presented in Fig. 2 are interchanged, leading to those in insets (i) of Figs. 3(a) and 3(b). The existence of modes is less surprising for these configurations, since they do follow the simple index-guiding intuition and do not rely on the presently introduced mechanism. The effective-index method can again be employed using for the central slice the SPs A or C [for Figs. 3(a) and 3(b), respectively] and for the outer slices the SP B, yielding the results shown in Fig. 3. The FDFD fundamental mode [insets (ii)] is again at most 1% away from this estimate. Note that for Fig. 3(a) the conserved wave number β must be larger than that of the mode supported by the $\epsilon_{\rm low} - \epsilon_{\rm hi} - \epsilon_{\rm low}$ waveguide standing vertically on top of the substrate for the field to couple only to decaying modes in y. More interestingly, the modes in Fig. 3(b) exhibit for small enough d a frequency regime of negative group velocity [13], bounded by two points of zero group velocity at nonzero wave vector β that can be used to design very high-Q cavities of nanoscale size [16].

An important lesson is that the index-guiding mechanism rigorously relates to appropriate effective and not actual material indices. In all-dielectric structures the two follow the same trend, but this is not the case always in the presence of metals, allowing for the design of what are basically surface-plasmon effective-index-guiding waveguides, like the ones above. Note, also, that care should be taken when searching for guided modes of such structures, in that the correct way to interpret the concept that the dispersion line of a mode lies *above* or *below* another is to compare their effective indices $n_{\rm eff} = ck/\omega$ at a *fixed frequency* ω and not the other way around, so perhaps the terms *left* and *right,* respectively, seem more appropriate.

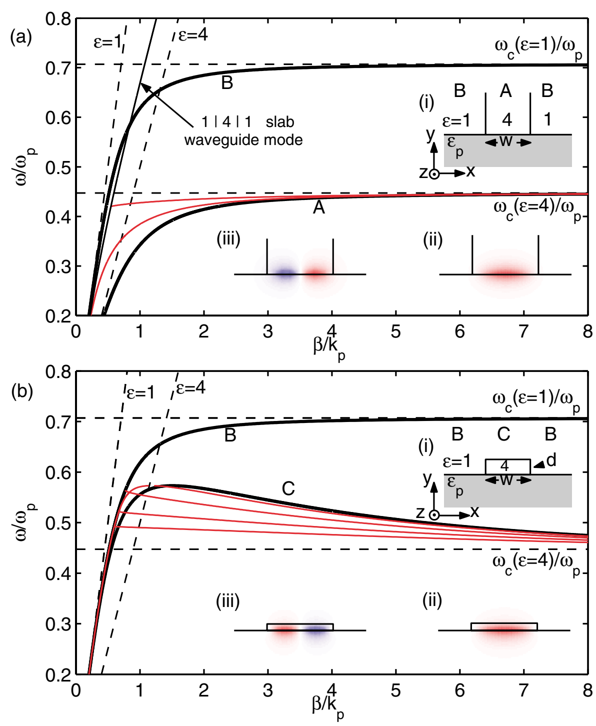

FIG. 3 (color). ω-β diagrams (red curves) for SP-based waveguide structures [insets (i)] with $w/\lambda_p = 0.25$ and $d/\lambda_p = 0.02$ and the H_x component of their first two modes at (a) $\omega/\omega_p = 0.444$ and (b) $\omega/\omega_p = 0.47$ [insets (ii) and (iii)].

The new class of waveguides presented here has features that could greatly impact the field of nanophotonics by being able to shrink light in all (spatial, temporal, and energy) scales. At the very high k values close to ω_c, the characteristic longtitudinal length and the transverse modal profile have sizes in the nanoscale, allowing for very high device compactness. The fact that the group velocity can become arbitrarily small by decreasing the core thickness is a very important attribute that can be used to significantly enhance nonlinearities or gain in devices, and thus to reduce their required operational power [17]. Furthermore, the amazing feature that this is achievable over a large bandwidth and with small group velocity dispersion implies that these waveguides can slow down and shrink ultrashort pulses without introducing distortion to them, thereby allowing for exciting promises in the fields of ultrafast optics, optical memories, and quantum computing [11].

An issue arising is whether light could be efficiently coupled into or out of these waveguides over their entire large bandwidth of operation. This should be feasible, since by adiabatically tapering the size of the waveguide core its modal dispersion curve can be brought into broadband alignment with that of a regular waveguide mode, and this is the key requirement for all coupling mechanisms.

The most important concern relating to the feasibility of surface-plasmon optics is that metallic structures exhibit high losses at optical wavelengths. The intrinsic loss of conducting materials stems from inelastic scattering mechanisms, namely, the predominant electron-phonon scattering, which can be suppressed only by cooling, and electron-electron scattering, which is negligible compared to the first at room temperatures. Additional loss mechanisms are those due to elastic scattering, as from impurities or imperfections of the crystal, dictating the need for very clean samples, and from the metal crystal boundaries, which can be very important if the geometry of the conductor has features of length scale smaller than the mean free path ($l \simeq 3\ \mu$m at $T = 300\,^\circ$K for copper) [13,18]. Here lies the advantage of the currently presented plasmonic waveguide design, in that it does not suffer from boundary scattering, since it involves only a large bulk and completely unpatterned metallic substrate, limiting thus the loss only to its intrinsic (electron-phonon) part, which can be decreased by lowering temperature. By using again the Drude model $\epsilon_p(\omega) = 1 - \omega_p^2/(\omega^2 + i\gamma\omega)$ to account for losses, a calculation for the planarly layered structures of Fig. 1 showed that their propagation characteristics stay intact up to large k values, while absorption loss increases as group velocity decreases and temperature increases. Specifically, for copper ($\omega_p \simeq 5 \times 10^{15}$ rad/s) at the frequency where the group velocity reaches $\simeq 0.1c$ the loss is $\simeq 5.8$ dB/μm at room temperature ($T = 300\,^\circ\mathrm{K} \Rightarrow \gamma \simeq 5 \times 10^{13}$ rad/s [18]) and much lower $\simeq 5.8 \times 10^{-4}$ dB/μm at liquid He temperature ($T = 4\,^\circ\mathrm{K} \Rightarrow \gamma \simeq 5 \times 10^8$ rad/s [18]), while for $\simeq 0.01c$ these numbers are $\simeq 72$ dB/μm and $\simeq 72 \times 10^{-4}$ dB/μm for the two temperatures, respectively. Lower losses might also be achievable by working with polaritonic materials.

We are deeply grateful to Miloš Popović for providing his finite-difference frequency-domain mode solver and thank Professor Franz X. Kärtner for his helpful comments. This work was supported in part by the DARPA Research Contract No. FA8750-04-1-0134 and also by the Materials Research Science and Engineering Center program of the National Science Foundation under Grant No. DMR-9400334.

*Electronic address: aristos@mit.edu

[1] J. D. Joannopoulos, R. D. Meade, and J. N. Winn, *Photonic Crystals: Molding the Flow of Light* (Princeton University Press, Princeton, NJ, 1995).
[2] Q. Xu, V. R. Almeida, R. R. Panepucci, and M. Lipson, Opt. Lett. **29**, 1626 (2004).
[3] H. Raether, *Surface Plasmons* (Springer-Verlag, Berlin, 1988).
[4] J. Takahara, S. Yamagishi, H. Taki, A. Morimoto, and T. Kobayashi, Opt. Lett. **22**, 475 (1997).
[5] P. Berini, Opt. Express **7**, 329 (2000).
[6] J.-C. Weeber, Y. Lacroute, and A. Dereux, Phys. Rev. B **68**, 115401 (2003).
[7] T. Nikolajsen, K. Leosson, I. Salakhutdinov, and S. I. Bozhevohyi, Appl. Phys. Lett. **82**, 668 (2003).
[8] M. Hochberg, T. Baehr-Jones, C. Walker, and A. Scherer, Opt. Express **12**, 5481 (2004).
[9] S. I. Bozhevolnyi, J. Erland, K. Leosson, P. M. W. Skovgaard, and J. M. Hvam, Phys. Rev. Lett. **86**, 3008 (2001).
[10] S. A. Maier, P. G. Kik, H. A. Atwater, S. Meltzer, E. Harel, B. E. Koel, and A. A. G. Requicha, Nat. Mater. **2**, 229 (2003).
[11] J. T. Mok and B. J. Eggleton, Nature (London) **433**, 811 (2005).
[12] G. Lenz, B. J. Eggleton, C. K. Madsen, and R. E. Slusher, IEEE J. Quantum Electron. **37**, 525 (2001).
[13] E. N. Economou, Phys. Rev. **182**, 539 (1969).
[14] J. J. Burke, G. I. Stegeman, and T. Tamir, Phys. Rev. B **33**, 5186 (1986).
[15] D. Marcuse, *Theory of Dielectric Optical Waveguides* (Academic Press, San Diego, 1991), 2nd ed.
[16] M. Ibanescu, S. G. Johnson, D. Roundy, Y. Fink, and J. D. Joannopoulos, Opt. Lett. **30**, 552 (2005).
[17] M. Soljačić and J. D. Joannopoulos, Nat. Mater. **3**, 211 (2004).
[18] C. Kittel, *Introduction to Solid State Physics* (Wiley, New York, 1996), 7th ed.